Spatial Periodic Perturbation of Turing Pattern Development Using a Striped Mask

Igal Berenstein, Milos Dolnik,* Anatol M. Zhabotinsky, and Irving R. Epstein

Department of Chemistry and Volen Center for Complex Systems, MS 015, Brandeis University, Waltham, Massachusetts 02454

Received: July 16, 2002; In Final Form: April 1, 2003

We study the influence of the intensity of light and the wavelength of an imposed parallel striped mask on the development of striped Turing patterns. Depending on the ratio $R = \lambda_F/\lambda_P$ of the wavelength of the mask to the wavelength of the natural pattern and on the amplitude of forcing, stripes develop parallel or perpendicular to the orientation of the mask. For R near 1.5 or 3, zigzag patterns develop. When weak forcing is applied, stripe splitting is observed for R near 2. For strong forcing, stripe splitting occurs over a wider range of R, and two sequences of splitting are observed when $R = 4$. At large R, fingers of spreading patterns develop, which propagate and reconnect to form stripes perpendicular to the mask orientation.

1. Introduction

The study of pattern formation in chemical and biological systems far from thermodynamic equilibrium is a central aspect of nonlinear science. Pattern-forming processes in homogeneous reaction−diffusion systems may be classified according to the instabilities that give rise to three different types of patterns: (i) spatially homogeneous and periodic in time; (ii) spatially periodic and stationary in time; (iii) periodic in both time and space.[1] Patterns that are stationary in time and periodic in space (type ii) are dubbed Turing patterns (TP) after Alan Turing, who, half a century ago, predicted their existence and their importance in morphogenesis.[2]

The chlorine dioxide−iodine−malonic acid (CDIMA) reaction, is a widely employed reaction−diffusion system for the study of TP.[3] Depending on the reaction conditions, the TP arrange themselves in stationary patterns of spots, stripes or a mixture of the two. Spots typically occur as regular patterns of hexagons, though they often exhibit defects that break the hexagonal symmetry. The natural development of striped TP never results in ordered symmetric patterns with stripes aligned along a single direction. Typical striped TP can rather be described as a combination of short striped segments with an arbitrary orientation, often referred to as labyrinthine patterns. In this work, we study striped TP formation under spatial periodic forcing, utilizing illumination of the thin gel layer where the TP form.

The majority of previous studies have focused on the asymptotic states of TP and little attention has been devoted to the growth dynamics.[4] This dynamics is particularly important in the case of spatial temporal forcing. The photosensitivity of the CDIMA system[5] can be used to control and modulate stationary TP,[6,7] as well as to create well-organized hexagonal patterns[7,8] and rhombic patterns.[7] Recently, we have studied temporal forcing of TP and found resonances in TP suppression.[6] We have also performed spatial periodic forcing of hexagonal TP using illumination through a mask with hexagonal symmetry and found that this forcing is effective in removing defects and producing ordered symmetric patterns.[8]

Other systems, including one with Bénard−Marangoni convection[9] and a nonlinear optical system,[10] that present stationary patterns have been subjected to spatial periodic forcing. Spatial entrainment of Turing-like patterns formed during polymerization of acrylamide in the methylene blue−sulfide system has also been studied.[11] The patterns in these systems display hexagonal symmetry, and in all of them, entrainment and frequency locking occur. In ref 10, the dynamics of defect motion has also been studied.

In this paper, we study a different symmetry (stripes), and we follow the dynamics of forced TP evolution.

2. Experimental Arrangement

The CDIMA reaction is carried out in a thermostated (4°C) one-sided continuously fed unstirred reactor (CFUR).[4,8] The CFUR consists of a 2% agarose gel (Fluka, 0.3 mm thickness and 25 mm diameter) placed between a glass impermeable window and a feeding chamber, a continuously fed stirred tank reactor (CSTR). A cellulose nitrate membrane (Whatman, with pore sizes 0.45 μm, thickness 0.12 mm) is placed beneath the gel to enhance contrast of patterns. To provide rigidity to the gel and to separate the gel from the intensively stirred feeding chamber, an anapore membrane (Whatman, pore size 0.2 μm, impregnated with 4% agarose gel, overall thickness 0.10 mm) is placed underneath the cellulose nitrate membrane.

Three solutions are fed into the feeding chamber using a Rainin peristaltic pump. One solution contains I_2 (Aldrich); the second is a mixture of malonic acid (MA, Aldrich) and poly(vinyl alcohol) (PVA, Aldrich, average molecular weight 9000−10000); the third contains chlorine dioxide, prepared as described in ref 12. PVA is a color indicator for triiodide ions, and it also diminishes the effective diffusivity of iodide, which is a requirement for the Turing patterns.[2] Each of the input solutions contains 10 mM sulfuric acid. After mixing, the concentrations inside the feeding chamber are (before any reaction takes place) as follows: $[I_2]_0 = 0.4$ mM, $[MA]_0 = 1.8$ mM, $[ClO_2]_0 = 0.14$ mM, $[PVA]_0 = 10$ g/L. The residence time of reagents in the feeding chamber is 240 s.

A 300 W quartz halogen lamp is used for illumination. A mask is placed in front of the light source, and its image is focused on the gel. The mask consists of a gray-scaled pattern of parallel stripes. The gray scale level, $0 \le GL \le 255$, along one direction (x) is designed as a simple sinusoidal function $GL = 128[1 + \cos(2\pi x/\lambda_M)] - 1$, where λ_M is the wavelength

* Corresponding author.

10.1021/jp026546k CCC: $25.00
Published on Web 05/08/2003

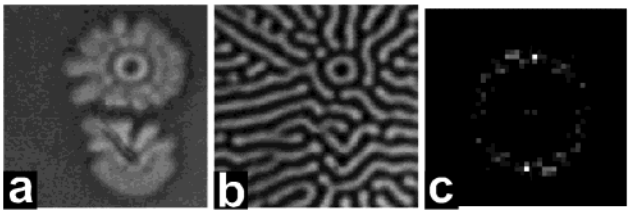

Figure 1. Development of Turing pattern after suppression of a naturally formed striped pattern by strong illumination: (a) spreading of a "flower pattern", snapshot taken 35 min after illumination is turned off; (b) "stationary" Turing pattern, snapshot taken 2 h after illumination is applied; (c) Fourier spectrum of pattern shown in panel b. The intensity of the analyzing light is 0.6 mW/cm^2. Snapshot area is 5 mm $\times$ 5 mm; frequency range of the Fourier spectrum is $\pm$4.2 mm^{-1}.

of the mask stripe pattern. The gray scale pattern is imprinted on a transparency, and the intensity of the transmitted light through the mask is determined. The relationship between the light intensity and the spatial x-coordinate of the projected image is then

$$I = I_0\left[1 + \sin\left(\frac{2\pi x}{\lambda_F}\right)\right]^2/4 \qquad (1)$$

where I_0 is the light intensity transmitted through the most transparent part of the mask, where GL = 255. We select λ_F, the forcing wavelength (wavelength of the mask image projected on the gel layer), as our control parameter. Two crossed polarizers are employed to control the light intensity. A Pulnix CCD videocamera equipped with a Hamamatsu camera controller is used for image acquisition.

3. Experimental Results

At the beginning of an experiment, we let TP develop spontaneously without external forcing and the wavelength of a stationary TP, λ_P, is evaluated from the Fourier spectrum (λ_P = 0.45 $\pm$ 0.02 mm). Formation of stationary Turing patterns typically takes at least 8 h after the start of an experiment.

The illumination mask is chosen so that the ratio of the forcing wavelength λ_F to λ_P corresponds to a desired ratio R:

$$R = \lambda_F/\lambda_P \qquad (2)$$

The spontaneously formed TP are suppressed by strong uniform homogeneous illumination (70 mW/cm^2 intensity, 5 min duration). As a result of this illumination, the iodine concentration and [SI_3^-] decrease in the entire illuminated area, and the uniform "white" state replaces the TP. If the light is turned off after the pattern suppression and no additional illumination is applied, the iodine concentration replenishes itself and the concentration of SI_3^- gradually increases, as documented by the color changes in the gel. Within 2$-$3 min after the end of illumination, the white (low [SI_3^-]) state changes to a dark (high [SI_3^-]) state in the previously illuminated area. After 15$-$20 min, white spots appear at random locations and serve as germs of new TP. These germs grow and spread into the surrounding area, forming flowerlike patterns.[4] Within approximately 2 h, a stationary TP is formed (Figure 1). Hence, the stationary pattern develops much faster after the suppression of TP than at the start of the experiment.

A different scenario of TP development is observed when, after suppression of TP by uniform illumination, a mask is placed between the light source and the gel and illumination is applied through the mask. The growth dynamics and the symmetry of the stationary TP depend on the light intensity I_0 and the forcing wavelength λ_F. We use two different levels of light intensity I_0, which we refer to as weak and strong forcing. The ratio R is varied from 0.8 to 8.0. We investigate both the growth dynamics and the stationary (asymptotic) state of TP under illumination. We also study the relaxation dynamics and the stationary states after the illumination is switched off.

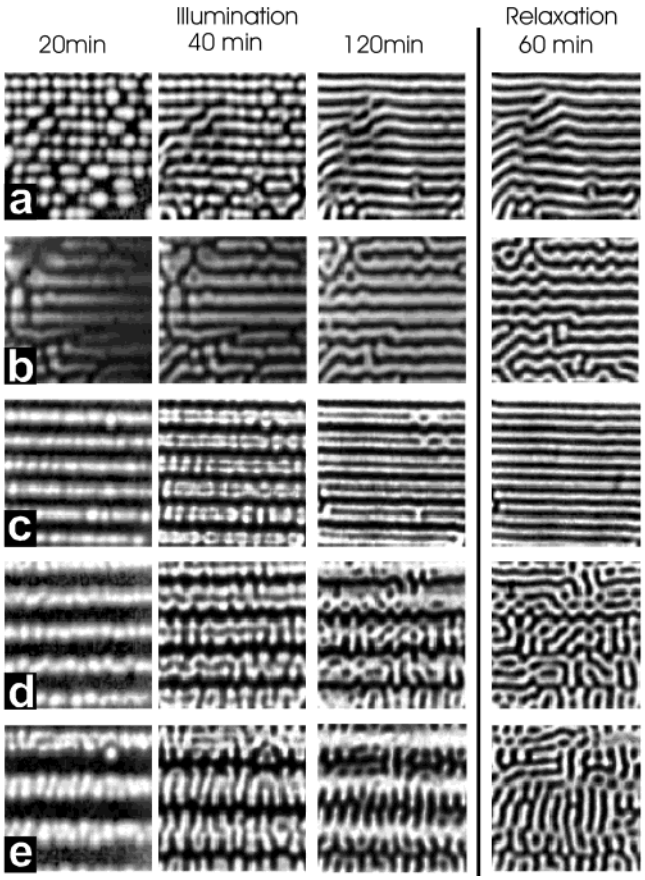

Figure 2. Pattern development during and after illumination through a mask at low intensity of illumination, I_0 = 12 mW/cm^2, and wavelength ratios (a) R = 1.1, (b) R = 1.4, (c) R = 1.9, (d) R = 2.9, and (e) R = 4. Snapshot area is 5 mm $\times$ 5 mm.

3.1. Weak Forcing. After suppression of the naturally formed striped TP by strong uniform light, a mask is placed between the light source with significantly reduced light intensity (I_0 = 9.6 mW/cm^2) and the gel. The gel layer is illuminated for 2 h with a light intensity profile described by eq 1. During the first few minutes of spatial illumination, the white state is replaced by the dark state in the entire area, as in the case of relaxation without external forcing. This observation indicates that the light intensity is too weak to noticeably alter this part of the relaxation process. Other stages of the growth dynamics, however, are affected by the external forcing, and the development of TP is determined by the wavelength of the mask image, λ_F. We study the growth dynamics of TP with weak forcing for the range R = 1.0$-$4.0.

When R is near unity (Figure 2a, R = 1.1), soon after the start of illumination, in those regions of the gel where the most intense light is applied, the consumption of iodine by the photochemical reaction leads to formation of white spots. As the spots grow, they merge and form a pattern of modulated stripes (Figure 2a, first two snapshots). The stripe modulation gradually diminishes, and eventually an ordered unmodulated striped TP becomes the asymptotic state (Figure 2a, third snapshot). Defects in the pattern symmetry appear owing to small heterogeneities in the gel. This stationary pattern is

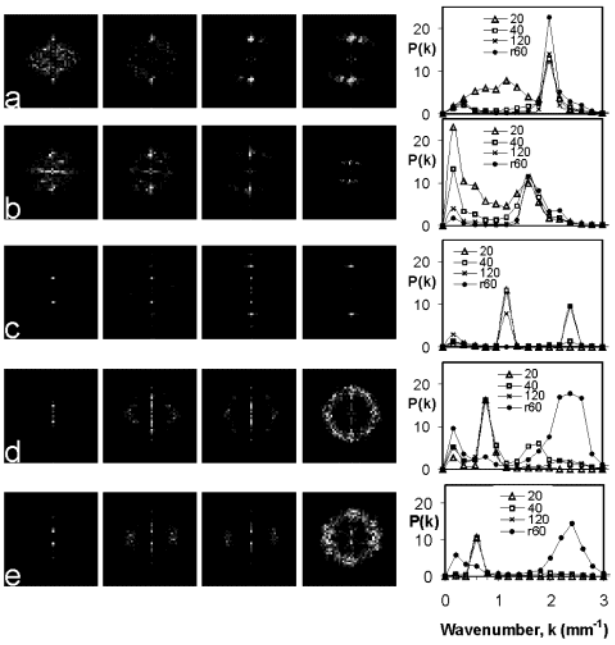

Figure 3. Two-dimensional Fourier spectra of snapshots shown in Figure 2. First four columns correspond to snapshots in Figure 2. The last panel represents the wavenumber distribution $P(k)$ in percent averaged over azimuthal angle. Legend numbers in the panel indicate time in minutes from the beginning of illumination; $r60$ is the data series corresponding to the fourth column in Figure 2. Frequency range shown is ± 4.2 mm^{-1}.

typically obtained within 2 h of illumination, and no further changes are observed if illumination is continued at the same light intensity.

To compare stationary patterns with and without spatial forcing and to investigate the relaxation of the forced state, we turn the light off and record the changes in TP formation. The last snapshot in Figure 2a, taken 60 min after the light is turned off, shows a pattern that undergoes no further visible changes after this time, and thus we consider it as a stationary pattern. The forcing wavelength λ_F is maintained by the pattern even after the external forcing is removed, as shown by the two large peaks in the Fourier spectrum corresponding to $\lambda_F = 0.50$ mm (Figure 3a).

For $R = 1.4$ (Figure 2b), the growth dynamics of TP is slightly different. We again observe the emergence of white spots together with narrow white stripes in the most intensely illuminated region. As the width of the white stripes increases with time, the stripes become unstable and a zigzag pattern forms. The largest peak in the Fourier spectrum is found at a wavenumber that corresponds to $\lambda_F = 0.63$ mm. The zigzag formation is detected in the spectrum by a growing amplitude at $k = 1/\lambda_P = 1/0.45$ mm^{-1}. Nevertheless, the dominant pattern orientation is still defined by the stripe mask. After the light is turned off, the pattern changes only slightly and develops a more pronounced zigzag modulation (Figure 2b, last snapshot), which is seen as a further increase in amplitude around $1/\lambda_P$ (Figure 3b).

When $R \approx 2$ (Figure 2c, $R = 1.9$), the initial growth is similar to that shown in Figure 2b; narrow white stripes appear, and their width gradually increases (Figure 2c, first snapshot). After about 30 min, the white stripes "split" as black stripes form in their central regions. In this way, the pattern adjusts its wavelength to be near its "natural" wavelength. The Fourier spectrum (Figure 3c) shows this splitting as the emergence of a new peak at the wavenumber corresponding to λ_P. Soon after

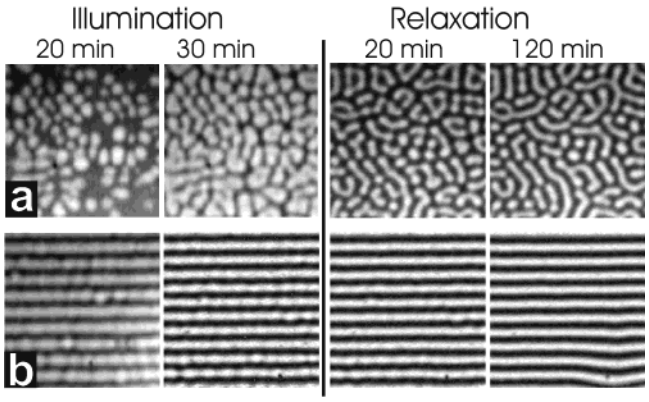

Figure 4. Pattern development for strong illumination, $I_0 = 23.6$ mW/cm^2, for $R =$ (a) 0.8 and (b) 1. Note that for $R = 0.8$ no alignment with the mask is obtained whereas for $R = 1$ the pattern aligns with the mask. Area shown is the same as that in Figure 2.

the forcing ceases and the pattern undergoes relaxation, the subharmonic peak disappears as the pattern rearranges into a well-ordered striped TP with the single characteristic wavenumber $1/\lambda_P$.

For $R \approx 3$ (Figure 2d, $R = 2.9$), a narrow white stripe develops first in the most intensely illuminated area and then spreads nonuniformly. Some stripes split, while other areas display finger growth perpendicular to the mask stripe orientation. (Figure 2d, second and third snapshots). The least illuminated area forms separation lines for this mixed pattern of fingers and stripes, and the Fourier spectra display major peaks at the forcing wavenumber. After the illumination is turned off, the pattern fills the whole area and resembles the spontaneously formed pattern. However, differences can be detected in the Fourier spectrum. The spectrum of the initially illuminated pattern after relaxation consists of several major peaks arranged along a circle. The location of these peaks indicates three main directions of stripe orientation (Figure 3d, last snapshot): (i) horizontal, as a result of splitting; (ii) vertical, from finger growth; (iii) diagonal, arising from interactions between splitting and finger growth. The spontaneously formed stripes, in contrast, occur in arbitrary directions, and the FFT does not display any preferred orientation of these patterns.

For $R \approx 4$ (Figure 2e, $R = 3.8$), each illuminated white stripe undergoes finger growth along its entire length. Fingers spread perpendicular to the forcing stripe orientation. The Fourier spectra of the stationary illuminated pattern display major peaks along the horizontal (mask stripe) direction, but soon after the light is turned off the fingers connect, resulting in formation of vertical stripes (Figure 2e, last snapshot).

3.2. Strong Forcing. Pattern formation and recovery after TP suppression by uniform light are affected more significantly by light of intensity $I_0 = 23.6$ mW/cm^2 with a profile given by eq 1. In the strongly illuminated area, the white state never turns into the dark state because the iodine that is formed and diffuses into this area is immediately consumed by the photodissociation reaction. In the less illuminated area, the concentration of $[SI_3^-]$ quickly replenishes and the white state is converted to the dark state. After 30 min of illumination, the pattern becomes stationary, and we turn the light off to follow the relaxation process.

When $R \leq 0.8$, the pattern development resembles that obtained by illumination with uniform light of intensity $I_0/2$, that is, no alignment with the mask is observed. The first two snapshots in Figure 4a show emerging white spots at random locations. After the illumination is turned off, stripes develop

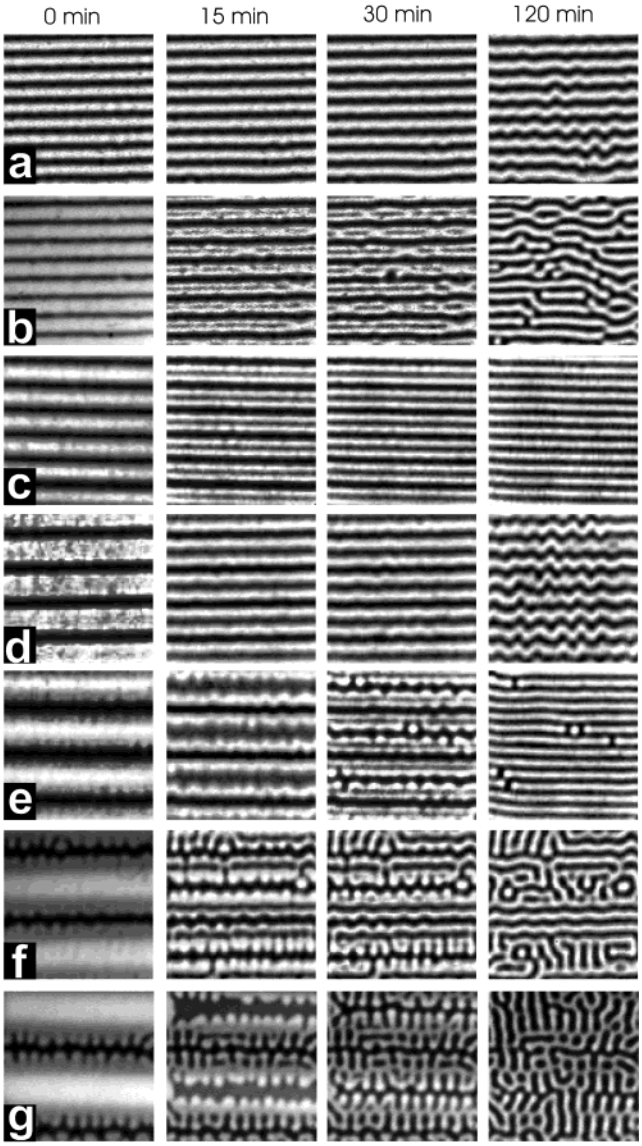

Figure 5. Relaxation of patterns after strong illumination, $I_0 = 23.6$ mW/cm^2 for wavelength ratios (a) $R = 1.4$, (b) $R = 1.6$, (c) $R = 1.9$, (d) $R = 2.9$, (e) $R = 4$, (f) $R = 6$, and (g) $R = 8$. Time on top indicates number of minutes after illumination is turned off.

without any preferred orientation (last snapshot in Figure 4a).

For $1 < R < 1.5$, the stationary TP under illumination and their relaxation resemble the behavior observed with weak forcing. When $R \approx 1$, the pattern remains practically unchanged when the light is turned off (Figure 4b). For $R = 1.4$, the stationary pattern under illumination consists of stripes with the orientation and wavelength of the mask image. Once the light is turned off, these stripes become unstable and a zigzag pattern develops (Figure 5a).

When $R > 1.5$, the imposed stripes start to break during relaxation. Figure 5b displays this process for $R = 1.6$. After stripe splitting, the wavelength of the newly formed stripes is 0.35 mm, significantly shorter than the wavelength of the natural pattern. For this reason, the splitting is relatively slow, and the imposed stripe does not split along its whole length. After 30 min of relaxation (Figure 5b, third snapshot), the predominant wavelength is still the wavelength of the mask. Later during the relaxation, the stripes rearrange and adjust their wavelength to 0.5 mm (Figure 5b, fourth snapshot). The stripes are mainly oriented along the mask, but because of the wavelength rearrangement this orientation is not perfect and the Fourier

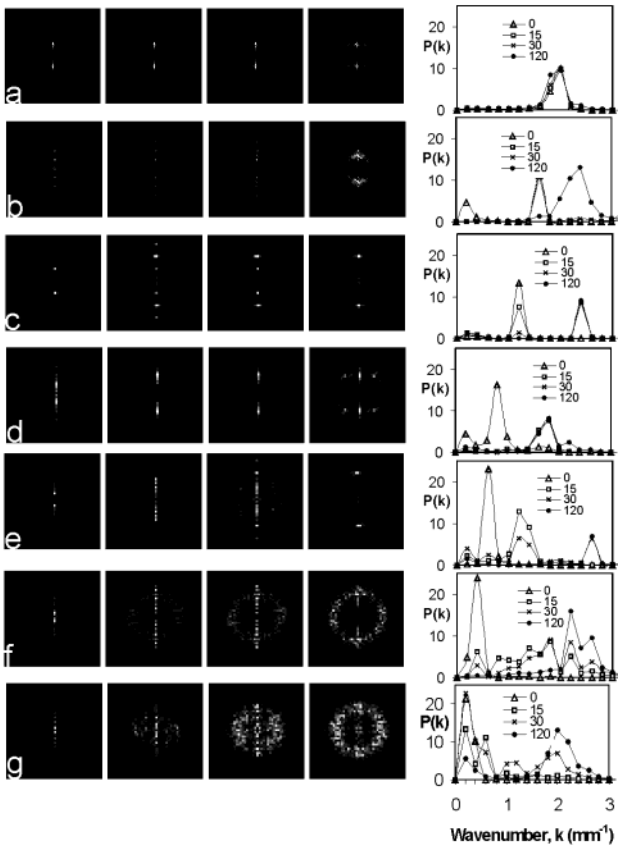

Figure 6. Fourier spectra of snapshots from Figure 5. The last panel represents the wavenumber distribution $P(k)$ averaged over azimuthal angle.

spectrum shows some scatter around the main peaks (Figure 6b, last snapshot). When $R = 1.9$, the stripes imposed by forcing split in two, and the final pattern is perfectly ordered with a wavelength close to λ_P (Figure 5c).

When $R \approx 3$, the pattern development differs from that observed for weak forcing. Illumination produces stationary stripes with the wavelength of the mask. After the illumination is removed, the stripes split in two in less than 15 min. The resulting wavelength is unstable (it is 50% longer than λ_P), and a zigzag pattern similar to that found with $R = 1.4$ develops (Figure 5d, cf. Figure 5a).

For $R \approx 4$, the stripes split after 15 min of relaxation (Figure 5e, second snapshot). The new stripes have wavelength $\lambda_F/2$, and as the white area grows and spreads, the stripes split again (Figure 5e, third snapshot), yielding a wavelength equal to that of the natural pattern. This pattern remains well-ordered and parallel to the orientation of the mask.

When $R \approx 6$, the behavior is more complex. The growth of stripes is not as homogeneous as that for smaller values of R. Within 15 min after the illumination is removed, the stripes have already split twice (Figure 5f, second snapshot). Stripes formed in regions of low light intensity are well aligned with the mask, but the "inner" stripes develop fingers. These fingers grow (Figure 5f, third snapshot) and collide to form perpendicularly oriented stripes. Eventually, the pattern becomes a mixture of stripes oriented along the mask and perpendicular short stripes (Figure 5f, last snapshot)

For $R \approx 8$, the pattern recovery leads primarily to formation of fingers (Figure 5g, first snapshot), as the imprinted stripes split and fingers develop perpendicular to the mask orientation (Figure 5g).

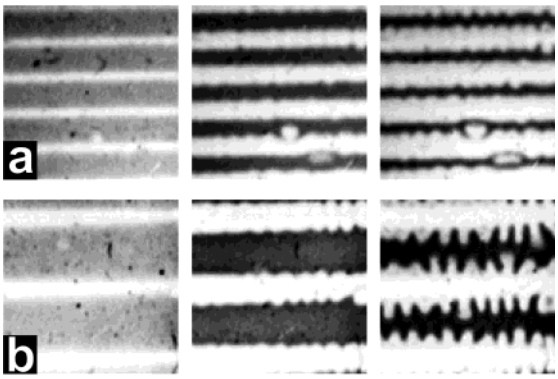

Figure 7. Pattern development during illumination with "on−off" mask with 25% transparent area for $I_0 = 30$ mW/cm^2 : (a) $R = 3$; (b) $R = 6$. First, second, and third snapshots taken at 10, 20, and 30 min of illumination, respectively.

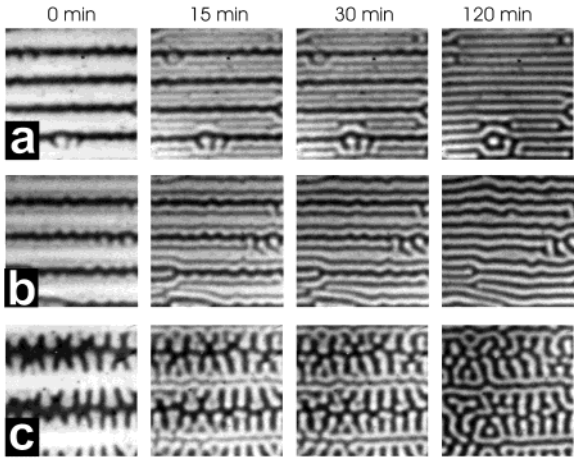

Figure 8. Relaxation of patterns after strong illumination with "on−off" mask with 25% transparent area, $I_0 = 30$ mW/cm^2: (a) $R = 3$; (b) $R = 4$; (c) $R = 6$.

3.3. "On−Off" Mask. The details of pattern formation depend on the initial width of the imprinted white stripe and upon its growth during development. To study the effect of the imprinted profile on pattern evolution, we employ not only masks with sinusoidal profiles but also striped masks with "on−off" (rectangular) profiles. With such masks, a constant light intensity is applied in the "on" (transparent) area and essentially no illumination reaches the gel in the "off" area of the mask. We investigate this "on−off" mask for wavelength ratios $R = 3$ and larger. Two types of "on−off" mask are used: one with the transparent part occupying $^1/_4$ of the wavelength (narrow stripe illumination); the other with the transparent part equal to $^3/_4$ of the wavelength (wide stripe illumination). The procedure corresponds to strong forcing with light intensity $I_0 = 23.6$ mW/cm^2.

With narrow stripe masks, iodine formation is inhibited in the illuminated area, while in the dark area the iodine concentration slowly increases. The concentration of SI_3^- gradually increases, as visualized by an increase in contrast with time in the snapshots shown in Figure 7. Narrow imprinted stripes of low iodine concentration first follow the mask profile (Figure 7a, first snapshot) but then expand (second and third snapshots). When $R > 4$, the white stripes develop fingers as they spread into the "dark" areas (Figure 7b).

Figure 8 illustrates the dynamics of relaxation after illumination with the narrow stripe mask. When $R \approx 3$, soon after the illumination is turned off, each white stripe splits into three narrow stripes (Figure 8a). For $R \approx 4$, the stripes also split in three, but the central stripe is broader than the side stripes (second and third panels in Figure 8b). With time, the central wide stripes become narrower, and the narrow stripes expand. Finally, all stripes have approximately the same width (Figure 8b, last snapshot). Using a mask with $R \approx 6$ results in well-developed fingers soon after illumination (Figures 7b and 8c). These fingers grow, while the central illuminated area splits (Figure 8c, second and third snapshots). After 2 h of relaxation, the fingers are still clearly visible, and a few have connected to form perpendicular stripes. The orientation of the pattern is mainly perpendicular to the orientation of the mask.

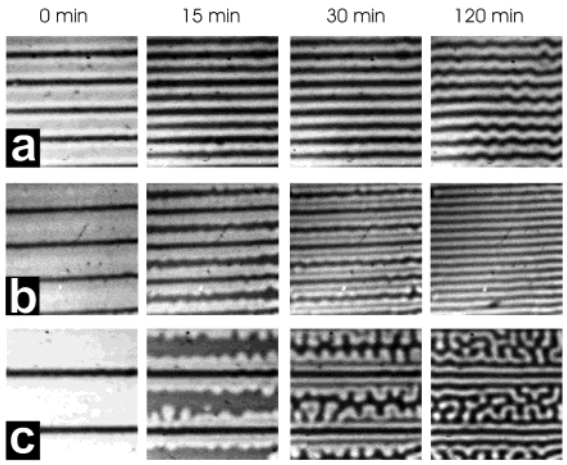

Figure 9. Relaxation of patterns after strong illumination with "on−off" mask with 75% transparent area, $I_0 = 30$ mW/cm^2: (a) $R = 3$; (b) $R = 4$; (c) $R = 6$.

After illumination with masks with wide transparent stripes, the imposed patterns show no fingering. The spreading of the low iodine zones is homogeneous. The relaxation process is similar to the one observed with sinusoidal masks. In Figure 9, relaxation sequences after forcing with masks with $R \approx 3$, 4, and 6 are shown. Parts a and b of Figure 9 strongly resemble parts d and e of Figure 5, respectively.

Figure 9c shows the nonuniform growth of stripes for $R \approx 6$. The relaxation process is again similar to the one observed with sinusoidal masks. Within 15 min after the removal of illumination, the stripes formed in the area near the boundaries of the illumination are well aligned with the mask. The "inner" stripes develop fingers, which grow (Figure 9c, third snapshot) and collide. Eventually, the pattern becomes a mixture of stripes oriented along the mask and a labyrinthine pattern. The area occupied by the stripes oriented along the mask in Figure 9c (last snapshot) is larger than that in Figure 5f.

4. Simulations

We employ a two-variable model that includes the effect of illumination:[6a]

$$\frac{\partial u}{\partial t} = a - u - 4\frac{uv}{1+u^2} - w + \nabla^2 u$$

$$\frac{\partial v}{\partial t} = \sigma\left[b\left(u - \frac{uv}{1+u^2} + w\right) + d\nabla^2 v\right] \qquad (3)$$

Here u and v are the dimensionless concentrations of $[I^-]$ and $[ClO_2^-]$, respectively; a, b, d, and σ are dimensionless parameters. In our simulations, we fix $a = 12.1$, $b = 0.26$, $d = 1.07$, and $\sigma = 50$, which results in the formation of striped TP analogous to those obtained in experiments. The rate of the photochemical reaction, $w = w(x)$, is a periodic function of the

x-coordinate and is independent of the *y*-coordinate, so the simulations mimic the experimental illumination of TP through a striped mask. In our simulations, we use either the sinusoidal profile,

$$w = w_0[1 + \cos(2\pi x/\lambda_F)]/2 \quad (4)$$

or the "on−off" profile,

$$w = w_0 \quad \text{for} \quad 0 < x \le r_{on}\lambda_F \,(\text{mod}\,\lambda_F)$$
$$w = 0 \quad \text{for} \quad r_{on}\lambda_F < x \le \lambda_F \,(\text{mod}\,\lambda_F) \quad (5)$$

Here $r_{on} \in (0,1)$ is the fraction of each wavelength for which the forcing is "on". For integration, we utilize the Euler method with fixed step size 0.001 time units and periodic boundary conditions. As initial conditions, we set u and v to their unstable steady-state values and add a small random perturbation to u at each spatial point.

5. Results of Simulations

To mimic the experiments, we use two different levels of the photochemical reaction rate. For weak forcing, we set $w_0 = 0.5$, and for strong forcing, $w_0 = 2.0$. The ratio R is varied from 0.8 to 8.0. As in the experiments, we analyze both the growth dynamics and the stationary state of TP under forcing.

After the forced pattern becomes stationary (the system is in an asymptotically locked state), we set $w = 0$ and investigate the relaxation dynamics and stationary state after the illumination is switched off. We first describe the results for sinusoidal forcing profiles, and then we summarize our simulations with "on−off" profiles.

5.1. Weak Forcing with Sinusoidal Stripe Profile. When R is near unity (Figure 10a, $R = 1.2$), then soon after the initiation of forcing, white stripes quickly form in the most intensely illuminated areas. The asymptotic state is an ordered striped TP with wavelength λ_F (Figure 10a, second snapshot). Small random perturbations applied initially do not affect the pattern symmetry, so the pattern is regular. If the forcing is applied for longer times, no further pattern development is observed. The removal of forcing does not affect the pattern significantly: the contrast changes slightly, but the symmetry and the wavelength remain unchanged (Figure 10a, last snapshot). For larger values of R, the simulated dynamics of TP development and relaxation display different scenarios. For $R = 1.5$ (Figure 10b), white stripes with wavelength λ_F are imprinted in the area with the most intense forcing. After the forcing is turned off, the stripes become unstable and a zigzag pattern forms (Figure 10b, last snapshot). When $R = 2$ (Figure 10c), the initial growth is similar to that shown in Figure 10b (first snapshot), but later the stripes split into two (Figure 10c, second snapshot), enabling the pattern to adjust its wavelength to the "natural" wavelength. After the forcing is removed, the pattern undergoes relaxation and stripes of equal width develop. For $R = 3$ (Figure 10d), the initial random perturbation leads to disordered pattern formation. One can detect the forcing stripe imprinting in the early stages of TP development (Figure 10d, first snapshot), but it becomes less visible as time goes on (second snapshot). After the forcing is removed, stripes with more or less arbitrary orientation develop (last snapshot). When R is increased to 4, an analogous scenario is observed (Figure 10e).

5.2. Strong Forcing with Sinusoidal Stripe Profile. With strong forcing, the imposed pattern is imprinted soon after the forcing is applied and remains essentially unchanged with time

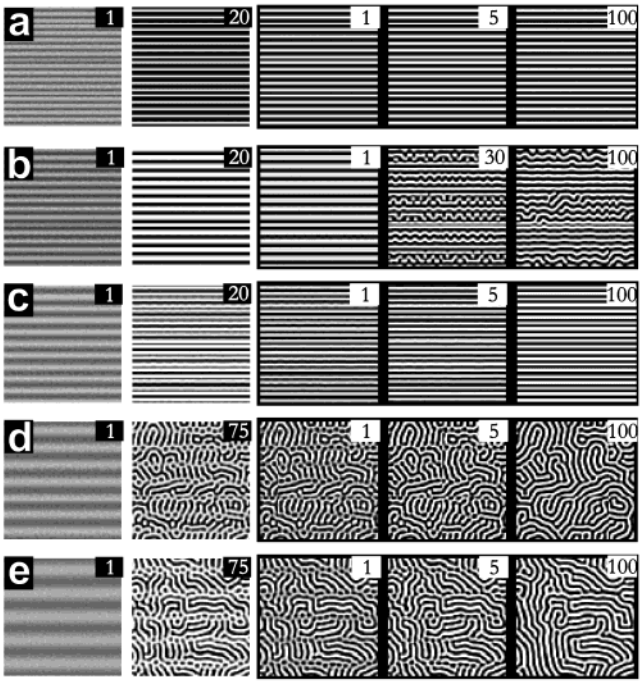

Figure 10. Simulations of pattern development with weak forcing using sinusoidal profile of stripes, $w_0 = 0.5$ for wavelength ratios $R =$ (a) 1.2, (b) 1.5, (c) 2.0, (d) 3.0, and (e) 4.0. Gray levels show dimensionless concentration of iodide: black corresponds to maximum value and white to minimum. First two snapshots with white background in each row are taken during forcing; number indicates time in dimensionless time units (tu) from the beginning of forcing. Second snapshot is taken at the end of forcing period and displays a stationary pattern with forcing. Last three snapshots with black background in each row are taken after the forcing is turned off, and numbers indicate tu elapsed after forcing is turned off.

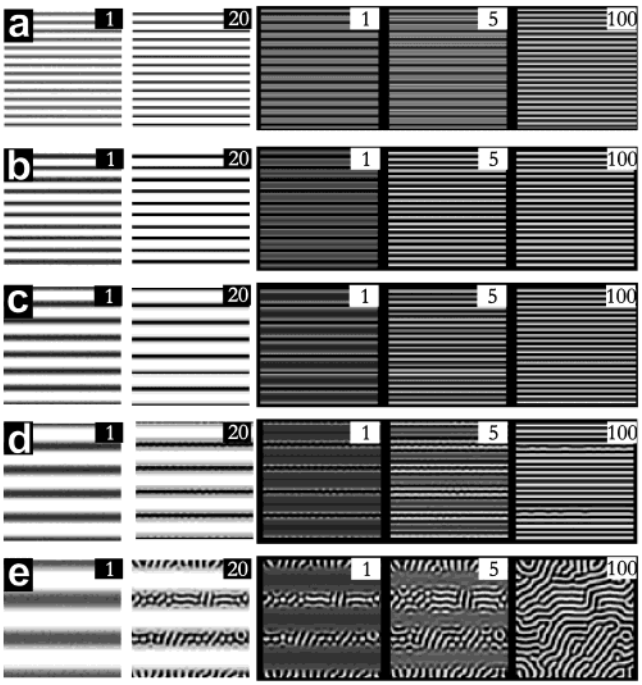

Figure 11. Simulations of pattern development with strong forcing using sinusoidal profile of stripes, $w_0 = 2.0$ for wavelength ratios $R =$ (a) 1.5, (b) 2.0, (c) 3.0, (d) 4.0, and (e) 6.0.

when R is relatively small ($0.8 < R \le 3$, Figure 11a, first two snapshots). For $R = 1.2$, the imprinted pattern of stripes remains unchanged after the forcing is eliminated and the pattern

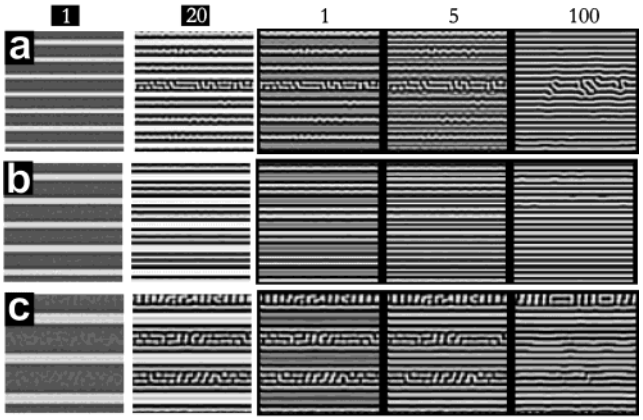

Figure 12. Simulations of pattern development with on−off profile of narrow stripes, $r_{on} = 0.25$ for wavelength ratios $R =$ (a) 3.0, (b) 4.0, and (c) 6.0.

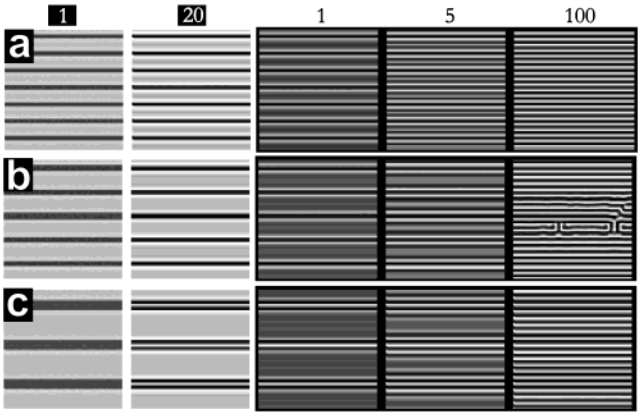

Figure 13. Simulations of pattern development with on−off profile of wide stripes, $r_{on} = 0.75$ for wavelength ratios $R =$ (a) 3.0, (b) 4.0, (c) 6.0.

maintains the forcing wavelength λ_F, as in the case of weak forcing (see Figure 10a). When $R = 1.5$, the imprinted wavelength λ_F is unstable for the unforced system, and the imprinted stripes split (Figure 11a) during relaxation. When strong forcing is applied, the initial random perturbation is obscured, and the pattern attains the mask orientation with no zigzag instability developing. The stationary stripe pattern has wavelength $\lambda_F/2$, which is 25% shorter than the natural pattern wavelength λ_P. When $R = 2$ (Figure 11b), a similar scenario occurs; during the relaxation period, the stripe splits and the pattern becomes stationary as it attains a wavelength equal to λ_P. When $R = 3$ (Figure 11c), the white stripes split in two early in the relaxation period and later a third stripe emerges between these two, yielding a wavelength for the stationary pattern of $\lambda_F/3$, which again corresponds to λ_P.

Pattern development under spatial forcing proceeds differently when $R > 3$. For $R = 4$, for example, wide stripes form first and then narrow stripes gradually form on each side of the wide stripes (Figure 11d, second snapshot). The width of the narrow stripes is nonuniform because they arise from amplification of a random initial perturbation. When the forcing is turned off, the narrow stripes retain their shape and color, that is, $[I^-]$ is relatively constant in this area. On the other hand, the wide stripes display significant changes in iodine concentration, and two additional stripes emerge in each one, resulting in a new stationary pattern consisting of ordered stripes with wavelength λ_P.

For $R = 6$ (Figure 11e), wide stripes form in the most illuminated area, while in the least illuminated region a "natural" pattern of randomly oriented stripes gradually develops. After the forcing is turned off, the wide stripes go into the dark state, and the "natural" pattern gradually spreads into this area. The final stationary pattern possesses wavelength λ_P.

5.3. "On−Off" Forcing. Figures 12 and 13 display the results of simulations with "on−off" profiles of narrow and wide stripe forcing, respectively. When narrow stripe forcing is applied ($r_{on} = 0.25$) then the forcing stripes are quickly imprinted. The dark (nonilluminated) area is relatively large for $R \geq 3$ and thus a pattern starts to develop in this region. For $R = 3$, the gap between imprinted stripes is too wide to fit one stripe and too narrow to fit two parallel stripes, so a zigzag pattern forms. When $R = 4$, two parallel stripes fill the dark area. For $R = 6$, many short stripes gradually emerge in the dark area. Once the forcing is turned off, the pattern rearranges; typically, a pattern of parallel stripes with defects emerges as the stationary pattern. The wavelength of these patterns is λ_P. The defects arise from the random initial conditions, and the number of defects increases with the amplitude of the initial random perturbation. When $R = 3$ (Figure 12a), the zigzag pattern of stripes gradually gives way to "straight" stripes as the system relaxes. When $R = 4$, the final pattern is a well-ordered striped pattern without defects (Figure 12b), while when $R = 6$, the defects rearrange into short perpendicular stripes (Figure 12c).

In the case of wide stripe forcing ($r_{on} = 0.75$), the imprinted stripes occupy most of the area. When $R \approx 6$, additional narrow stripes emerge in the nonilluminated area (Figure 13c, second snapshot). After the forcing is removed, the imprinted stripes split into three (Figure 13a, $R = 3$), four (Figure 13b, $R = 4$), and five (Figure 13c, $R = 6$) stripes with wavelength λ_P.

6. Discussion and Conclusions

We have studied both experimentally and numerically how the spatial periodic illumination of TP during development affects pattern formation and selection. Under our experimental conditions in the absence of forcing, the system displays flowerlike growth dynamics,[4] leading to formation of striped TP. The stripes form in random directions, and the 2D Fourier spectrum of a stationary TP consists of peaks on a circle, the radius of which defines the wavenumber of a "natural" pattern.

When illumination is applied to a uniform state, the areas illuminated most intensely become germs of a new TP. When weak illumination is applied, or when forcing is removed in the case of strong illumination, these germs spread into the surrounding area. With relatively small wavelength ratios R, the surrounding area is rather restricted and flat wave fronts spread into the less illuminated areas. As the growing stripe width increases, it may become unstable after reaching a critical size. We then observe stripe splitting with formation of two stripes of half the wavelength of the original wide stripe. If the new wavelength is stable, no other adjustment is needed and a stationary pattern forms. Because the front moves perpendicular to the mask stripe orientation and the growing stripe pattern splits in the middle, the stationary TP attains the orientation of the forcing mask. If further adjustment of the wavelength is needed, then another stripe splitting may occur. If the new wavelength is unstable, but further splitting would produce another unstable wavelength, then a zigzag pattern will develop.

If R is large, there is enough space around the imprinted germs of TP for fingers of spreading patterns to develop instead of a flat front wave. These fingers propagate perpendicular to the stripes and reconnect to form stripes at 90° to the mask orientation. Separation lines between growing stripes typically

form in the area with the lowest intensity of illumination. In the case of stripe splitting, these separation lines between stripes remain unchanged even after the forcing is removed. In the case of finger growth, this area is invaded by reconnecting fingers.

Stripe splitting is observed for weak forcing only for a relatively narrow wavelength range, $R \approx 2$. For strong forcing, splitting is observed for a much wider range of R. The mask profile also plays an important role in pattern formation for larger forcing wavelengths. The strong forcing provides long-range ordering of TP within a large range of the ratio $R = \lambda_F/\lambda_P$. Weak forcing provides this ordering only for a narrow range of R.

Numerical simulations using a simple two-variable model in two spatial dimensions reproduce well many of the results observed in experiments, for example, stripe splitting and formation of zigzag patterns. The simulations also predict the TP symmetry and orientation for weak and strong forcing as R is varied. Some of the behavior observed in experiments was not obtained in simulations, for example, the "finger growth" seen in experiments is not found in the simulations. To reproduce this experimental observation, one may need to utilize a more detailed model with more dynamical variables or simulations of a 3D system with illumination on one side while the gel is fed from the other side.

To better mimic experimental conditions, a small random perturbation was added to the initial conditions in our simulations. Without the added noise, the simulations produce patterns well aligned along the direction of the forcing mask even for very weak forcing, which is in disagreement with our experimental observations. The amplitude of the random initial perturbation is not very important because it only affects the initial conditions before the external forcing takes over control of the pattern development. In the weakly and nonilluminated regions the amplitude of the random initial perturbation affects the rate of pattern development but not its final shape.

Pattern formation has been controlled by external spatial periodic forcing in other systems as well. For example, competition between intrinsic and topographically imposed patterns has been studied in Bénard−Marangoni convection.[13] When subjected to line (stripe) forcing, the convection cells organize along the imposed pattern, but contrary to our results on Turing pattern forcing, the Bénard−Marangoni convection cells use the perpendicular direction to adjust its wavelength to the external forcing.

Theoretical models of reaction−diffusion systems have been proposed to account for pattern formation in morphogenesis. Various mechanisms can describe skin pattern changes during growth. For example, skin patterns of mammals change proportionally with the size of the organism, and no readjustment occurs. On the other hand, the stripe pattern on the skin of the marine angelfish *Pomacathus* continuously rearranges during growth.[14,15] When the juveniles of *Pomacathus* are small, they typically have three stripes. As they approximately double in size, new stripes emerge between the original stripes, and the number of stripes doubles. A similar process repeats as the fish doubles in size again. The newly emerging stripes are thin and broaden with time.

In our experiments, we observe a similar scenario. Although our system has a fixed size, without any "growth", the stripes induced by external forcing with $R > 1.5$ can be maintained only when the illumination is on. After the illumination is turned off, the stripe pattern rearranges by the stripe-splitting mechanism. The stripe-splitting mechanism seems to be preferred when stripes develop and rearrange simultaneously across the whole system. An analogous stripe-splitting mechanism has also been obtained in a simple reaction−diffusion model with growing size.[15]

Another mechanism by which wavelength adjustment can be achieved, stripe addition, has not been observed in the present experiments, but it can occur in the CDIMA reaction−diffusion system. If the system grows only at one end and the stripe pattern is well established in the remainder so that it does not "stretch" as the system grows, then a new stripe is "added" in the "new" domain. This stripe addition mechanism has been demonstrated in simulations of the CDIMA reaction−diffusion system with controlled pattern formation and a moving boundary.[16]

Acknowledgment. This work was supported by the National Science Foundation and the W.M. Keck Foundation.

References and Notes

(1) Cross, M. C.; Hohenberg, P. C., *Rev. Mod. Phys*. **1993**, *65*, 851.
(2) Turing A. M. *Philos. Trans. R. Soc. London, Ser. B* **1952**, *237*, 37.
(3) (a) Rudovics, B.; Barillot, E.; Davies, P. W.; Dulos, E.; Boissonade, J.; De Kepper, P. *J. Phys. Chem. A* **1999**, *103*, 1790. (b) Epstein, I. R.; Lengyel, I. *Physica D* **1995**, *84*, 1. (c) Noszticzius, Z.; Ouyang, Q.; McCormick, W. D.; Swinney, H. L. *J. Phys. Chem*. **1992**, *96*, 6302.
(4) Davies, P. W.; Blanchedeau, P.; Dulos, E.; De Kepper, P. *J. Phys. Chem. A* **1998**, *102*, 8236.
(5) (a) Muñuzuri, A. P.; Dolnik, M.; Zhabotinsky, A. M.; Epstein, I. R. *J. Am. Chem. Soc.* **1999**, *121*, 8065. (b) Rabai, G.; Kovacs, K. M. *J. Phys. Chem. A* **2001**, *105*, 6167.
(6) (a) Horvath, A. K.; Dolnik, M.; Muñuzuri, A. P.; Zhabotinsky, A. M.; Epstein, I. R. *Phys. Rev. Lett*. **1999**, *83*, 2950. (b) Dolnik, M.; Zhabotinsky, A. M.; Epstein, I. R. *Phys. Rev. E* **2001**, *63*, 026101.
(7) (a) Ouyang, Q.; Gunaratne, G. H.; Swinney, H. L. *Chaos* **1993**, *3*, 707. (b) Gunaratne, G. H.; Ouyang, Q.; Swinney, H. L. *Phys. Rev E* **1994**, *50*, 2802.
(8) Dolnik, M.; Berenstein, I.; Zhabotinsky, A. M.; Epstein, I. R. *Phys. Rev. Lett.* **2001**, *87*, 238301.
(9) Semwogerere, D.; Shatz, M. F. *Phys. Rev Lett*. **2002**, *88*, 054501.
(10) (a) Neubecker, R.; Zimmermann, A. *Phys. Rev. E* **2002**, *65*, 035205-(R). (b) Neubecker, R.; Jakoby, O. Spatial synchronization of regular optical patterns. Preprint.
(11) Fecher, F.; Strasser, P.; Eiswirth, M.; Schneider, F. W.; Münster, A. F. *Chem. Phys. Lett.* **1999**, *313*, 205.
(12) *Handbook of Preparative Inorganic Chemistry*, 2nd ed.; Brauer G., Ed.; Academic Press: New York, 1963; Vol. 1, p 301.
(13) Ismagilov, R. F.; Rosmarin, D.; Gracias, D. H.; Stroock, A. D.; Whitesides, G. M. *Appl. Phys. Lett* **2001**, *79*, 439.
(14) Kondo, S.; Asai, R. *Nature* **1995**, *376*, 765.
(15) Painter, K. J.; Maini, P. K.; Othmer, H. G. *Proc. Natl. Acad. Sci. U.S.A.* **1999**, *96*, 5549.
(16) Kærn, M.; Satnoianu, R.; Muñuzuri, A. P.; Menzinger, M. *Phys. Chem. Chem. Phys.* **2002**, *4*, 1315.